A LIKELIHOOD-BASED FRAMEWORK FOR QUANTIFICATION OF BRAIN RECEPTOR PET STUDIES IN THE PIXEL DOMAIN

Z. Jane Wang, Zsolt Szabo[2], Zhu Han, Jozsef Varga[3], and K. J. Ray Liu

Department of Electrical and Computer Engineering, University of Maryland, College Park
[2] Department of Radiology, Johns Hopkins University Medical Institutions, MD
[3] Department of Nuclear Medicine, University of Debrecen, Hungary

ABSTRACT

Quantification of receptor binding studies obtained with PET is complicated by tissue heterogeneity in the sampling image elements pixels and voxels. This effect is caused by a limited spatial resolution of the PET scanner. On the other hand, spatial heterogeneity is often essential in understanding the underlying receptor binding process. In this paper, we propose a likelihood-based framework in the pixel domain for quantitative imaging with or without the input function. Radioligand kinetic parameters are estimated together with the input function. The parameters are initialized by a subspace-based algorithm, and further refined by an iterative likelihood-based estimation procedure. The performances of the proposed scheme is examined by simulations. Real brain PET data are also examined to show the performance in determining the time activity curves and the underlying factor images.

1. INTRODUCTION

New functional imaging techniques represent powerful tools for the visualization and elucidation of important molecular mechanisms [1]. For example, using positron emission tomography (PET) and a specific radioligand, the serotonin transporter (SERT) in the brain can be quantified to assess the integrity of serotonergic neurotransmission [2]. Compartmental analysis forms the basis for tracer kinetic modeling in dynamic imaging [3] and the region of interest (ROI) approach is widely used [4]-[6]. Invasive measurement of the input function from arterial blood samples represents a limited, but not negligible risk of complications including thrombosis, infection and nerve injury. Therefore, it is of great interest to estimate both the kinetic parameters and input function simultaneously and in a noninvasive fashion. Only a few works for this purpose have been reported, including a Monte Carlo method called simulated annealing [5], the nonlinear least square method in [4], and three blind identification schemes [6]. The present work addresses PET quantification with or without knowledge of the input function.

An important shortcoming of ROI-based approaches is that tissue response in a ROI is assumed homogeneous. In reality, each ROI, even each image pixel is composed of multiple tissue components. The minimal number of such components is 3: one representing vascular activity, one representing displaceable binding to the receptor of interest (called specific binding), and one representing nondisplaceable binding to other tissue components (called nonspecific binding). Limited time of imaging, limited sampling rate, and increasing image noise in PET typically do not permit application of a more complex tissue response model. The factor analysis (FA) approach has been explored for separation of these three components [7]. However, the resulting factors are unrelated to the compartmental model and the underlying receptor binding process; in addition, the factors are not quantitative and not reproducible which limits their diagnostic usage. In this work, we propose a new approach in the pixel domain while keeping the compartmental modeling approach. We propose to construct a likelihood-based framework for estimating the spatial/temporal patterns of tissue binding with and without the measured input function.

2. SYSTEM MODEL AND FORMULATION

We focus on the two-compartment model since it provides stable and reproducible parameter estimates. However, the schemes developed in this paper can be generalized further and applied to more complex models. As in [1], we have

$$\begin{aligned} c_f(t) &= k_{1f} a_f(t), \text{ with } a_f(t) = c_p(t) \otimes e^{-k_{2f}t}, \quad (1) \\ c_s(t) &= k_{1s} a_s(t), \text{ with } a_s(t) = c_p(t) \otimes e^{-k_{2s}t}, \end{aligned}$$

where $\otimes$ denotes the convolution operation, the time $t \geq 0$, $k_{2f} > k_{2s} > 0$, $c_f(t)$ and $c_s(t)$ are the radioactivity in the fast and slow turnover pools, respectively; $c_p(t)$ is the input function; k_{1f} and k_{2f} (also k_{1s} and k_{2s}) are the washin and washout rate constants. The dynamics of each pixel i within the organ (i.e. brain) is as

$$c_m(i,t) = k_{1f}(i)a_f(t) + k_{1s}(i)a_s(t) + v_p(i)c_p(t) + \epsilon(i,t), \quad (2)$$

for $i = 1, ..., N$, with $k_{1f}(i)$ and $k_{1s}(i)$ being the local permeability parameters associated with pixel i; $v_p(i)$ means the plasma volume; and $\epsilon(i,t)$ is the noise term. Tracer kinetics are often represented by a serial compartmental model. We use a parallel model here since its micro- and macro-parameters are identical. In case of a serial model the macroparameters need to be transformed to obtain the microparameters. Let $\mathbf{a}_f$, $\mathbf{a}_s$, and $\mathbf{c}_p$ be the discrete versions sampled uniformly every T seconds, we have

$$\mathbf{a}_f \triangleq \mathbf{H}(k_{2f})\mathbf{c}_p; \quad \mathbf{a}_s \triangleq \mathbf{H}(k_{2s})\mathbf{c}_p, \quad (3)$$

where $\mathbf{H}(k_{2f})$ (similarly $\mathbf{H}(k_{2s})$) is a nonsymmetric Toeplitz matrix with first column $[1, e^{-k_{2f}T}, e^{-k_{2f}2T}, ..., e^{-k_{2f}(P-1)T}]$, and T should be small enough to yield accurate result.

However, the PET images are generally acquired with increasing time intervals. Let $\mathbf{t} = \{t_1, t_2, ..., t_n\}$ indicate the arbitrary sampling times, we employ the linear interpolation to represent the measurements, meaning we have the discrete model

$$\mathbf{c}_m(i) = [c_m(i,t_1), ..., c_m(i,t_n)]^T = \mathbf{QAs}(i) + \epsilon(i), \quad (4)$$

0-7803-8388-5/04/$20.00

with $\mathbf{A} = [\mathbf{a}_f, \mathbf{a}_s, \mathbf{c}_p]$, $\mathbf{s}(i) = [k_{1f}(i), k_{1s}(i), v_p(i)]^T$, and the interpolation matrix $\mathbf{Q}$ is $n \times P$, with each row containing 1 or 2 non-zero elements determined by the mapping between the vector $\mathbf{t}$ and $[0, T, ..., (P-1)T]$.

Assume that the noise $\epsilon(i,t)$ is both temporally and spatially white Gaussian distributed, with zero mean and variance σ^2. The complete parameter set is $\theta = \{k_{2f}, k_{2s}, \mathbf{c}_p, \mathbf{s}(1), ..., \mathbf{s}(N), \sigma^2\}$ in our problem. Write $\mathbf{X} = [\mathbf{c}_m(1), \mathbf{c}_m(2), ..., \mathbf{c}_m(N)]$, we can derive the likelihood function $f(\mathbf{X}; \theta)$. With $\mathbf{A}$ is fixed, for each pixel i, the ML estimate of $\mathbf{s}(i)$ and σ^2 can be derived and substituted. Therefore, the set of parameters is $\theta_\mathbf{s} = \{k_{2f}, k_{2s}\}$ when knowing the input function (as measured), and $\theta_\mathbf{s} = \{k_{2f}, k_{2s}, \mathbf{c}_p\}$ for the case that the input function is not available. Our problem is formulated in the framework of likelihood testing as

$$\hat{\theta}_s = \arg \min_{\theta_s} \left\{ \sum_{i=1}^{N} ||\mathbf{c}_m(i) - \mathbf{Q}\mathbf{A}\hat{\mathbf{s}}(i)||^2 \right\} \triangleq \arg \min_{\theta_s} L(\theta_s), \tag{5}$$

with some constraints (e.g. $k_{2f} > k_{2s} > 0$). Therefore, our estimation problem is modelled as a high-dimensional optimization problem. In this paper, for comparison, we also employ RFSQP (Reduced Feasible Quadratic Programming) algorithm [8] to numerically solve the above constrained nonlinear optimization problem due to its efficiency.

3. PROPOSED SCHEME

We propose an integrated scheme: First, a subspace based algorithm is developed to obtain the initial estimates of the parameters. Secondly, with the initial guess, the iterative ML technique is applied to improve the estimation accuracy.

3.1. Case 1: Known Input Function

In this case, the plasma input function $c_p(t)$ is represented by a sequence of blood samples. We obtain the uniformly sampled $\mathbf{c}_p$ via the simple linear interpolation.

Subspace Based Algorithm
Based on the model in (4), we note that the covariance matrix is:

$$\begin{aligned} \mathbf{R} &= E\{\mathbf{c}_m(i)\mathbf{c}_m(i)^T\} = \mathbf{Q}\mathbf{A}\mathbf{D}_0\mathbf{A}^T\mathbf{Q}^T + \sigma^2\mathbf{I}_n \\ &= \mathbf{Q}_s\Lambda_s\mathbf{Q}_s^T + \sigma^2\mathbf{Q}_w\mathbf{Q}_w^T, \quad \text{with } \mathbf{D}_0 = E\{\mathbf{s}(i)\mathbf{s}(i)^T\}, \end{aligned}$$

where $\mathbf{Q}_s$ and $\mathbf{Q}_w$ consist of signal and noise eigenvectors respectively. Clearly, $\mathbf{D}_0$ has a full rank $M = 3$. Note that the potential signal is presented by $\mathbf{a}_s(\alpha) = \mathbf{Q}\mathbf{H}(\alpha)\mathbf{c}_p$. Therefore, using the orthogonal property of eigen-decomposition, we develop a MUSIC-like subspace-based algorithm as

$$S(\alpha) = \frac{1}{\sum_{m=M+1}^{n_s} |\mathbf{q}_m^T\mathbf{a}_s(\alpha)|^2}, \tag{6}$$

where $0 < e^{-\alpha} < 1$. Here we are particularly interested in the MUSIC(Multiple SIgnal Classification) algorithm because of its wide success in many areas [9]. Similar to MUSIC spectrum which exhibits peaks in frequency components, here the peaks correspond to the exponent parameters k_{2s} and k_{2s}. Due to the heavy noise in PET data, some peaks may not show up. Intuitively, we note that fast-flow component is clearer in early time images, while slow-flow component is demonstrated more clearly in images of the later stage. Therefore, we process the image sequences in a sliced-window manner to find all peaks, as illustrated in Fig. 1 for the later example of brain PET study.

Further Refinement
Though the above subspace based algorithm is generally accurate, we can further improve the accuracy by using $\hat{k}_{2s}$ and $\hat{k}_{2s}$ obtained above as the initial estimate and applying any standard nonlinear programming schemes to solve the 2-dimensional problem

$$\hat{\theta}_s = \{\hat{k}_{2f}, \hat{k}_{2s}\} = \arg \min_{\theta_s} \text{Tr}\{(\mathbf{I} - \mathbf{Q}\mathbf{A}(\mathbf{A}^T\mathbf{Q}^T\mathbf{Q}\mathbf{A})^{-1}\mathbf{A}^T\mathbf{Q}^T)\hat{\mathbf{R}}\} \tag{7}$$

after plugging the ML estimate of $\mathbf{s}(i)$'s.

3.2. Case 2: Unknown Input Function

In this case, $c_p(t)$ also needs to be estimated based on the pixel measurements $c_m(i,t)$'s. To reduce the parameter dimension of the problem, we consider a parametric model of the input function proposed in [10], having $c_p(t) = (a_1 t - a_2 - a_3)e^{\lambda_1 t} + a_2 e^{\lambda_2 t} + a_3 e^{\lambda_3 t}$. To remove the redundancy, we set $a_1 = 1$ and have

$$\mathbf{c}_p = \begin{pmatrix} {}^0_T e^{\lambda_1 T} & {}^1_{e^{\lambda_1 T}} & {}^1_{e^{\lambda_2 T}} & {}^1_{e^{\lambda_3 T}} \\ \vdots & \vdots & \vdots & \vdots \end{pmatrix} \begin{pmatrix} {}^1_{-a_2 - a_3} \\ {}^{a_2}_{a_3} \end{pmatrix} \triangleq \mathbf{B}(\lambda)\mathbf{b} \tag{8}$$

in which $\lambda_1 < \lambda_2 < \lambda_3 < 0$, with $\lambda = \{\lambda_1, \lambda_2, \lambda_3\}$. Now we note that the signal-matrix $\mathbf{A}$ is fully characterized by parameters k_{2f}, k_{2s},λ_j's, and a_j's, since

$$\mathbf{A} = [\mathbf{H}(k_{2f})\mathbf{B}(\lambda)\mathbf{b}, \mathbf{H}(k_{2s})\mathbf{B}(\lambda)\mathbf{b}, \mathbf{B}(\lambda)\mathbf{b}].$$

Subspace Based Algorithm
Our analysis on Laplace-transform shows that the signal sub-space $\mathbf{S}$ is characterized by exponential decaying signals and $te^{-\lambda_1 t}$, meaning that we have

$$\begin{aligned} \mathbf{c}_m(i) &= [\mathbf{f}_0(-k_{2f}), \mathbf{f}_0(-k_{2s}), \mathbf{f}_0(\lambda_1), \mathbf{f}_1(\lambda_1), \\ &\quad \mathbf{f}_0(\lambda_2), \mathbf{f}_0(\lambda_3)]\mathbf{c}(i) + \epsilon(i) = \mathbf{S}\mathbf{c}(i) + \epsilon(i), \end{aligned} \tag{9}$$

where the coefficient vector $\mathbf{c}(i)$ indicates the weight of each signal component at pixel i, and $\mathbf{f}_0(\alpha)$ and $\mathbf{f}_1(\alpha)$ are the values of $e^{\alpha t}$ and $te^{\alpha t}$ sampled at $\mathbf{t}$, respectively. Now we can write:

$$\hat{\mathbf{R}} = \mathbf{S}\mathbf{D}\mathbf{S}^T + \sigma^2\mathbf{I}_n, \text{with } \mathbf{D} = E\{\mathbf{c}(i)\mathbf{c}(i)^T\}, \tag{10}$$

Since the signals represented in $\mathbf{S}$ are coherent as a result of the convolution model in (2), there is a rank deficiency in matrix $\mathbf{D}$.

In radar direction finding applications, combining the ideas of spatial smoothing and array interpolation make it possible to restore the rank of the signal covariance matrix for arbitrary array geometries [12]. Since $\mathbf{S}$ is a Vandermonde matrix when uniformly sampled, we employ the similar idea: we form a single "virtual" uniformly spaced sampling time points, divide the exponent values into sectors, and design the best interpolation matrix for each sector in the least square sense; we then apply the smoothing technique by splitting the TACs into a number of overlapping sub-TACs with length n_s, and the covariance matrices based on sub-TACs are then averaged. Thus, we can make $\mathbf{D}$ with a full rank $M = 6$, and compute MUSIC-like algorithms as

$$S_0(\alpha) = \frac{1}{\sum_{m=M+1}^{n_s} |\mathbf{q}_m^T\mathbf{f}_0(\alpha)|^2}; \tag{11}$$

where $0 < e^{\alpha} < 1$. We use the constraints ($k_{2f} > k_{2s} > 0$ and $\lambda_1 < \lambda_2 < \lambda_3 < 0$) to help the mapping between the peaks and

the exponent parameters. Based on the mapping, several sets of the estimates of the exponent parameters can be used as parallel initial estimates. We need to further estimate the coefficients a_2 and a_3 by minimizing the cost function as defined in (5).

Iterative Likelihood Maximum (ILM)

Since any prior information (belief) should be helpful in improving the accuracy, we exploit the non-negative property of the underlying factor image coefficients (e.g. $k_{1f}(i) \geq 0$). With a fixed $\mathbf{A}$, estimating the factor coefficients $\mathbf{s}(i)$ equals to solve a constrained optimization problem

$$\hat{\mathbf{s}}(i) = \arg \min_{\mathbf{s}(i)} ||\mathbf{c}_m(i) - \mathbf{QAs}(i)||^2, \text{ subject to } \mathbf{s}(i) \geq 0, \quad (12)$$

via applying the Lagrange multiplier theorem. We then plug in this estimate into the cost in (5) when estimating the parameters θ_s.

We propose an iterative alternative, called the iterative likelihood maximization or iterative minimization, to further improve the estimation accuracy. The main idea, with its root in Alternative Projection (AP)[11], is to achieve multidimensional minimization by solving successive lower-dimensional minimization problems iteratively. At iteration $(k+1)$, the update of the estimate $\theta_s^{(k+1)}$ is obtained by solving the following one- or two-dimensional minimization problems: Update the ML estimates of the parameter pair (k_{2f}, k_{2s}) under constraints, while fixing all other parameters; update the ML estimates of the parameter pair (λ_2, a_2); then update the ML estimates of the parameter pair (λ_3, a_3); then update the ML estimates of the parameter λ_1, with subject to $\lambda_1 < \lambda_2^{(k+1)}$. These sub steps are iteratively applied until the convergence is achieved.

4. SIMULATIONS FOR UNKNOWN INPUT FUNCTION

The proposed scheme should accurately estimate the three factor TACs associated with the organ (i.e., $a_f(t)$); and it should locate the organ heterogeneity characterization reasonably accurate.

Let $\mathbf{y}$ and $\hat{\mathbf{y}}$ be the true and estimated factor TAC, respectively. We calculate the correlation coefficient (CC) between $\hat{\mathbf{y}}$ and $\mathbf{y}$. We also study the norm of the corresponding residuals defined as $(\hat{\mathbf{y}} - \mathbf{y})$, since it is desirable for an estimator to fit the real factor curve in a least-square sense. To make a fair comparison, we perform "centering" and "normalization" on the three factor TACs over time $\mathbf{t}$ before we calculate the above performance measures.

Considering a measure of adherence to the second objective above, we calculate the CC between the estimated factor image $\{\hat{k}_{1i}\}$ and the true one. In addition, we propose PM, the relative distance between the true and the estimated factor coefficients, as

$$PM_f = \frac{1}{N} \sum_{i=1}^{N} \frac{|\hat{k}_{1,f}(i) - k_{1,f}(i)|}{k_{1,f}(i)}. \quad (13)$$

The smaller PM is, the better performance in revealing the spatial heterogeneous structure.

We report simulation results for the case of unknown input function. The images are uniformly sampled every 15 seconds from 0 to 10 minutes. The input function $c_p(t)$ is generated from the parametric model proposed in [10]. The simulated organ phantom consists of three significantly-overlapped underlying factor images, where each factor image includes a light and a darker sub-region. The coefficients (e.g. $\{k_{1f}(i)\}$) are randomly drawn from one of the two uniform distributions. For instance, $\{k_{1f}(i)\}$ and $\{k_{1s}(i)\}$ are from the uniform distributions $U(0.1, 0.4)$ and $U(0.8, 1)$. The noise level is chosen as $\sigma^2 = 30$.

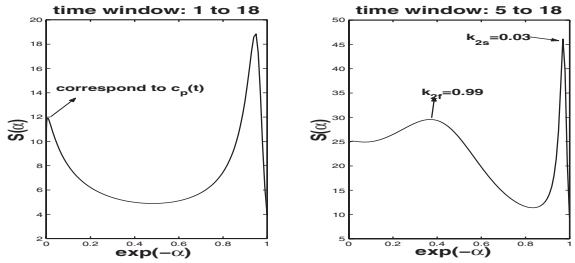

Fig. 1. An brain PET example of estimating the exponent parameters using MUSIC-like algorithm.

One example of the estimated factor TACs is shown in Fig. 2, where good matches are observed. We are particularly interested in the factor images which reveal the underlying spatial heterogeneity. We study the statistical behave of the correlation coefficient between the true and estimated factor images and the performance measure PM. Correspondingly, Table 1 shows their empirical means and standard deviations based on the estimate of factor images from 100 simulation runs. It is clear that the proposed scheme provides high accuracy in estimating the factor images. The high-dimensional numerical approach RFSQP, used as a performance bound here, requires high computational complexity, and it may not always converges and careful investigation has been taken in our simulation to provide the converged results. We note that the proposed scheme yields comparable performance to that of RFSQP in estimating the underlying factor images which demonstrate the spatial heterogeneity of each component.

5. REAL DATA CASE

We now examine the PET study of a healthy control subject obtained after intravenous injection of C-11 labelled DASB, a radioligand for the SERT. We used a GE Advance PET camera with an axial resolution (FWHM) of 5.8 mm, and an in plane resolution of 5.4 mm. 18 serial dynamic PET images were acquired during the first 95 minutes after injection using the following image sequence: four 15 sec frames, three 1 min frames, three 2 min frames, three 5 min frames, three 10 min frames, and two 20 min frames. All PET scans were reconstructed using the Ramp-filtered back-projection technique in a 128x128 matrix, with a transaxial pixel size of 2x2 mm. Arterial blood samples were withdrawn every 5-7 seconds during the first two minutes, then with increasing time intervals until the end of study 95 minutes post injection, and the input function was corrected for metabolized radioligand activity, as shown in Fig. 3(a).

We first consider knowing the input function. Fig. 3(a) shows the factor TACs estimated by the proposed scheme, where the factor curves are meaningful and follow compartmental kinetics. The reconstructed factor images are shown in Fig. 4, where the left image represents nonspecific binding and the right image appears to represent specific binding. Further, as typically in practice, the specific binding in the temporal and frontal cortex is lower than in the midbrain. We then examine the case of simultaneously estimating the input function too by plotting the estimated factor TACs and factor images in Fig. 3(b) and Fig. 5. We can see that the results match with the case of using the measured input function.

factor	fast	slow	input
CC	(0.962,0.041)|(0.955,0.100)	(0.996,0.005)|(0.980,0.010)	(0.980,0.016)|(0.968,0.015)
PM	(0.388,0.113)|(0.320,0.188)	(0.110,0.079)|(0.305,0.071)	(0.207,0.064)|(0.269,0.054)

Table 1. Performance of estimating the factor images, in terms of the mean and standard deviation of PM. Here the noise level $\sigma^2 = 30$.

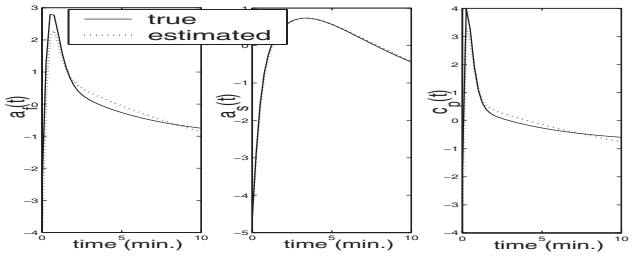

Fig. 2. The true and the estimated factor TACs in simulation.

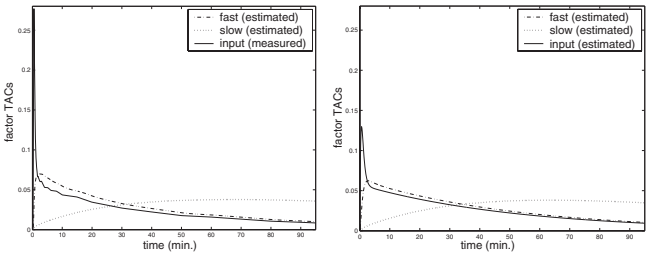

Fig. 3. The estimated factor TACs in brain PET study in the case of knowing the measured input function (left), and the case of estimating the input function simultaneously (right).

6. CONCLUSION

We developed a likelihood-based framework in the pixel domain for estimating the kinetic parameters and revealing the spatial and temporal characteristics, regardless whether the measured input function is available or not. We studied several performance measures to examine the results of the proposed scheme in estimating the three factor TACs, and in revealing the underlying spatial heterogeneous structures (e.g. the factor images). The results illustrate that the proposed scheme is able to quantify the binding parameters, it provides reliable estimations of factor TACs, and is very promising in examining the spatial heterogeneity in tissue dynamics on a pixel-by-pixel basis. Simulations show that the proposed scheme provides comparable performance to that of RFSQP, which serves as a performance bound in our estimation problem. Furthermore, we studied the result on brain PET data, and good performance was observed.

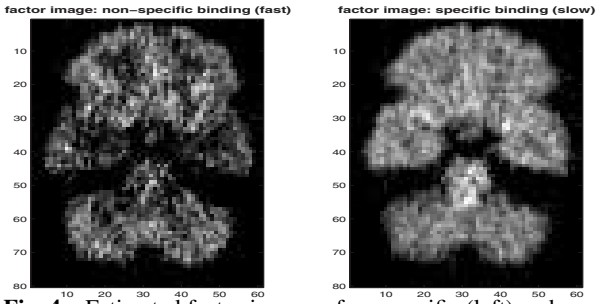

Fig. 4. Estimated factor images of nonspecific (left) and specific (right) binding from brain PET study using the measured input function.

7. REFERENCES

[1] Y. Zhou, S-C Huang, T. Cloughesy, C. K. Hoh, K. Black, and M. E. Phelps, "A Modeling-Based Factor Extraction Method for Determining Spatial Heterogeneity of Ga-68 EDTA Kinetics in Brain Tumors", *IEEE Trans. Nuclear Sci.*, vol. 44(6), pp. 2522-2527, 1997.

[2] L. Kerenyi, G. Ricaurte, D. Schretlen, U. McCann, J. Varga, W. Mahews, H. Ravert, R. Dannals, J. Hilton, D. Wong, and Z. Szabo, "Positron Emission Tomography of Striatal Serotonin Transporters in Parkinson's Disease", *Arch Neurol*, vol. 60, pp. 1223-1229, 2003.

[3] R. Gunn, R. Steve, and V. Cunningham, "Positron Emission Tomography Compartmental Models", *Journal of Cerebral Blood Flow and Metabolism*, vol. 21, no. 6, pp. 635-652, 2001.

[4] D. Feng, K. Wong, C. Wu, and W. Siu, "A Technique for Extracting Physiological Parameters and the Required Input Function Simultaneously from PET Image Measurements: Theory and Simulation Study", *IEEE Trans. Inform. Tech. Biomed.*, vol. 1, pp. 243-254, Dec. 1997.

[5] K. Wong, R. Meikle, D. Feng, and M. Fulham, "Estimation of Input Function and Kinetic Parameters Using Simulated Annealing: Application in a Flow Model", *IEEE Trans. On Nuclear Science*, vol. 49, no. 3, June 2003.

[6] D. Riabkov and E. Bella, "Estimation of Kinetic Parameters Without Input Functions: Analysis of Three Methods for Multichannel Blind Identification", *IEEE Trans. on Biomedical Eng.*, vol. 49, no. 11, Nov. 2002.

[7] H. Wu, C. Hoh, S. Huang et al, "Factor Analysis for Extraction of Blood Time-Activity Curves in Dynamic FDG-PET Studies", *J. Nucl Med*, vol. 36, no. 9, pp. 1714-1722, 1995.

[8] C. Lawrence, "A Computationally Efficient Feasible Sequential Quadratic Programming Algorithm", PhD thesis, ECE Dept., University of Maryland, 1998. (ISR-TR Ph.D 98-5.)

[9] H. Krim and M. Viberg, "Two Decades of Array Signal Processing Research", *IEEE Signal Processing Magazine*, pp. 67-93, July 1996.

[10] D. Feng, S. Huang, and X. Wang, "Models for Computer Simulation Studies of Input Functions for Tracer Kinetic Modeling with Positron Emission Tomography", *Int. J. Biomed. Comput.*, vol. 32, pp. 95-110, 1993.

[11] I. Ziskind and M. Wax, "Maximum Likelihood Localization of Multiple Source by Alternate Projection", *IEEE Trans. ASSP*, vol. 36, pp. 1553–1560, Oct. 1988.

[12] B. Friedlander and A. Weiss, "Direction Finding Using Spatial Smoothing With Interpolated Arrays", *IEEE Trans. on Aerospace and Electronic Systems*, vol. 28(2), pp. 574-587, 1992.

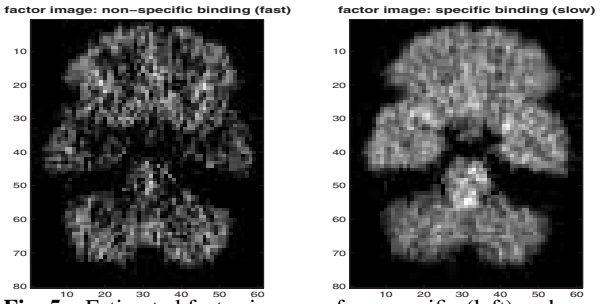

Fig. 5. Estimated factor images of nonspecific (left) and specific (right) binding from brain PET study with simultaneous estimation of the input function.